A SIMPLE AND ACCURATE METHOD FOR ESTIMATING THE STATOR WINDING REAL-TIME TEMPERATURE OF AIR-COOLED HYDROGENERATOR

by

Jiangtao YANG* * *and Zhenyu WANG

College of Electrical and Information Engineering, Hunan University, Changsha, China

Original scientific paper
https://doi.org/10.2298/TSCI220224120Y

In this paper, a novel and simple method is proposed for estimating the stator winding real-time temperature of the air-cooled hydrogenerator. Firstly, the structure and temperature characteristics of the hydrogenerator are analyzed. Then, a data-driven method for estimating the stator winding real-time temperature is proposed, and the implementation steps are illustrated in detail. Finally, the real-time temperature of the stator winding is estimated by the proposed method with different days, which is validated by the test. The result shows that the proposed method can well predict the temperature of the stator winding, which provides a new idea for the temperature measurement of the large hydrogenerator.

Key words: *data-driven, temperature, hydrogenerator, real-time*

Introduction

Hydropower resources have become an ideal energy source for electricity production due to their merits of cleanliness, no pollution to the environment, and recyclability [1]. A hydrogenerator is the core of the efficient use of water energy. Safe and reliable operation of the hydrogenerator is very important for the entire power station [2].

Temperature is an important indicator for the operation of hydrogenerator, which can reflect the operating state of the hydrogenerator. Too high operating temperature would shorten the operating life of the hydrogenerator, and even burn the hydrogenerator [3]. Hence, it is necessary to calculate and monitor the temperature distribution of hydrogenerator.

The temperature calculation methods of hydrogenerator mainly include lumped parameter thermal network (LPTN), finite element analysis (FEA) and CFD [4-6]. In LPTN, thermal resistance is related to the temperature and fluid conditions. Therefore, it is necessary to use fluid network to obtain the cooling flow distribution of the electrical machine to determine the convective heat transfer coefficient. The fluid distribution inside the electrical machine is relatively complicated, and it is difficult to accurately solve it with a simple fluid network, which limits the accuracy of LPTN [7]. The FEA can directly subdivide the physical model of the electrical machine, load the corresponding loss and the boundary conditions corresponding to each heat dissipation path, and then the detailed temperature distribution can be obtained. The results obtained are more intuitive and detailed than LPTN. However, consistent with LPTN, the heat transfer conditions on each boundary still need to be obtained

* Corresponding author, e-mail: yangjiangtao@hnu.edu.cn

with the help of fluid networks and empirical formulas, so there is no guarantee that the results are more accurate than LPTN [8]. The CFD can jointly model and solve the heat transfer entity and the cooling fluid inside and outside of the electrical machine. The fluid-flow state, the heat transfer coefficient of the wall surface and the temperature distribution inside the electrical machine can be solved at the same time. Therefore, it can completely replace the aforementioned fluid network and LPTN or FEM temperature rise models. Because there is no need to use empirical formulas to determine the heat transfer coefficient of each part, the result is more accurate [9]. However, CFD is usually used to analyze the steady-state temperature in the motor design process. The CFD is time-consuming for the calculation of steady-state temperature, needless to say the real-time temperature. Therefore, it is unsuitable to be used to analyze the real-time temperature of the hydrogenerator [10].

To monitor the real-time temperature, temperature sensors are usually adopted in the hydrogenerator. The temperature of the stator winding is the highest in the hydrogenerator [11]. Hence, the temperature sensors are usually installed in the middle of the stator winding. As time goes by, the temperature sensor gradually ages or even breaks down. It is difficult to replace the temperature sensor in the stator winding between the upper and lower coil bars. The stator winding needs to be removed from the hydrogenerator when replacing the sensor, which would delay power generation time, cause high maintenance costs, and may even damage the hydrogenerator. To save the cost and time, it is necessary to find a simple method for estimating the real-time temperature of stator winding.

Addressing this issue, a novel and simple method for estimating the stator winding real-time temperature of the air-cooled hydrogenerator is proposed in this paper. The temperature sensor is easy to install at the end of the stator winding and disassemble, and the temperature of the end of the stator winding is also a real-time physical quantity. If the relationship between the middle temperature and the end temperature can be found and the functional relationship between them can be fitted, then the temperature at the observation point of the stator winding can be estimated by the temperature at the end of the winding.

Model and temperature characteristics

In this work, the stator winding temperature of an 18.5 MW air-cooled hydrogenerator is analyzed. The analysed model of the hydrogenerator is illustrated and the relationship between the temperature and output power is investigated in this section.

Analysed hydrogenerator

Figure 1 shows the structure of the hydrogenator. The main parameters of the hydrogenerator are given in tab. 1. The cooling system of the hydrogenerator is shown in fig. 2. The heat dissipation path is: the cold air blown by the fan enters the radial ventilation holes of rotor yoke, the wind enters stator core through the radial ventilation holes of the yoke ring along the poles to cool the stator and rotor, the hot air flows along the vent hole of the frame ring plate behind the stator core yoke and enters the air cooler, and the cooled air is blown out by the fan and enters the radial ventilation holes of rotor yoke again.

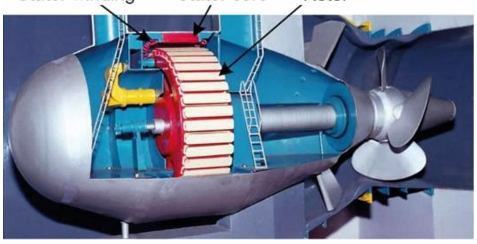

Figure 1. Structure of hydrogenerator [12]

Table 1. Main parameters of the hydrogenerator

Parameters	Value	Parameters	Value
Rated power [MW]	18.5	Rated voltage [V]	1050
Rated frequency [Hz]	50	Power efficiency	0.9
Stator Outer diameter [mm]	6400	Stator inner diameter [mm]	5960
Length of iron core [mm]	1040	Air-gap length [mm]	10
Rotor outer diameter [mm]	5940	Rotor inner diameter [mm]	5240
No. of stator slots	432	No. of pole-pairs	32
Length of vent [mm]	5	No. of stator vents	24
No. of bars in a slot	2	–	–

Temperature measuring point on stator winding

To illustrate the stator structure of the hydrogenerator, one stator slot of this machine is presented, as shown in fig. 3(a). To observe the temperature sensor of the stator winding, the cross-section of a stator slot along a-a1 is given in fig. 3(b). The temperature sensor PT100 is installed on a shim between two coil bars in a stator slot. The temperature measuring point is located in the middle of the generator winding.

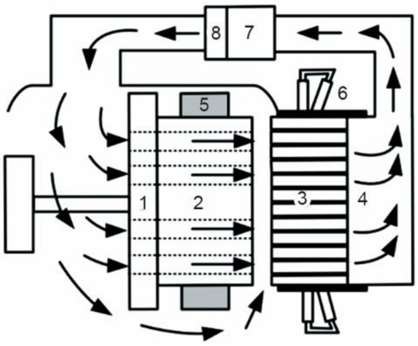

Figure 2. Air-cooling system;
1 – rotor yoke, 2 – rotor pole, 3 – stator core, 4 – air collector, 5 – field winding, 6 – stator winding, 7 –air cooler, 8 – fan

Temperature characteristics

The temperature of stator winding is directly affected by the output power of the hydrogenerator. The greater the power, the greater the loss. The loss of the hydrogenerator is dissipated in the form of heat, which causes the change of temperature in the stator winding, stator core, *etc*. Although the temperature of the stator winding is related to the hydrogenerator's power, their corresponding relationship is complex. Due to their different physical properties, the power, P, can change drastically in a short time, but the temperature, T, cannot. The relationship between the output power and stator winding temperature versus time can be described as fig. 4 [13]. After the power remains constant for enough time, if possible, under the premise

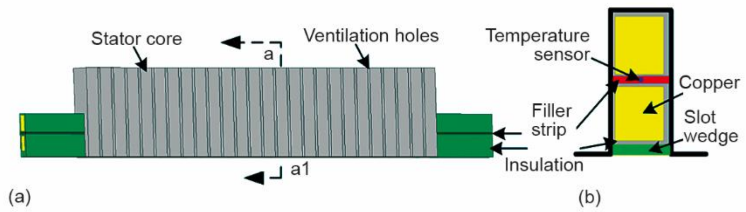

Figure 3. Temperature measuring point; (a) analysed model corresponding to a stator slot and (b) cross-section of a stator slot

of constant external conditions, the temperature of stator winding will tend to a stable value. When the power suddenly drops, based on the aforementioned analysis, the temperature of stator winding will decrease gradually and then become steady, and vice versa. Figure 5 shows the power and measuring point temperature in a period of time obtained by the monitoring system of the hydrogenerator. It can be found that the power changes much faster than the temperature of stator winding, which is in accordance with the theoretical analysis. Temperature variation lags behind power variation. The power of the hydrogenerator can change so frequently and abruptly that the winding temperature cannot keep up with it fast enough, as revealed in fig. 5. Therefore, the relationship between the power and the temperature of stator winding is obscure, complex, and time dependent. It is difficult to realize the real-time and relatively accurate estimation of measuring point temperature of the hydrogenerator by its power.

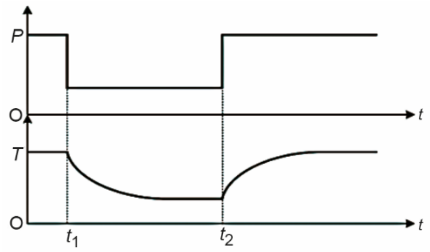

Figure 4. Relationship between power and temperature of stator winding

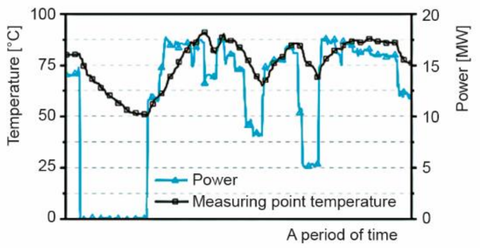

Figure 5. Power and measuring point temperature of the hydrogenerator

Proposed method to estimate temperature

As time goes by, the temperature sensor embedded in the middle of stator winding of the hydrogenerator will be damaged. Limited to the stator structure of hydrogenerator and the difficulty of assembly, the damaged temperature sensor is difficult to remove, and the new one cannot be installed in the original position. To estimate the observation point temperature of the hydrogenerator, a simplified method is proposed, which is explained in detail in the following.

Proposed method

To estimate the observation point temperature of the hydrogenerator, a temperature sensor is installed at the end of stator winding, as shown in fig. 6. The temperature sensor is attached to the winding surface, which is easy to maintain. The temperature of observation point of stator winding is obtained based on the temperature of the sensor installed at the end of stator winding. The flow-chart of the proposed method for estimating the winding temperature is given in fig. 7.

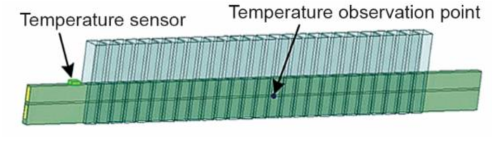

Figure 6. Temperature at the observation point

Data analysis

Originally, the hydrogenerator was equipped with several temperature sensors installed in the middle of the stator windings, which were evenly arranged along the circumferential direction. Eventually, one of the temperature sensors was damaged. The new temperature

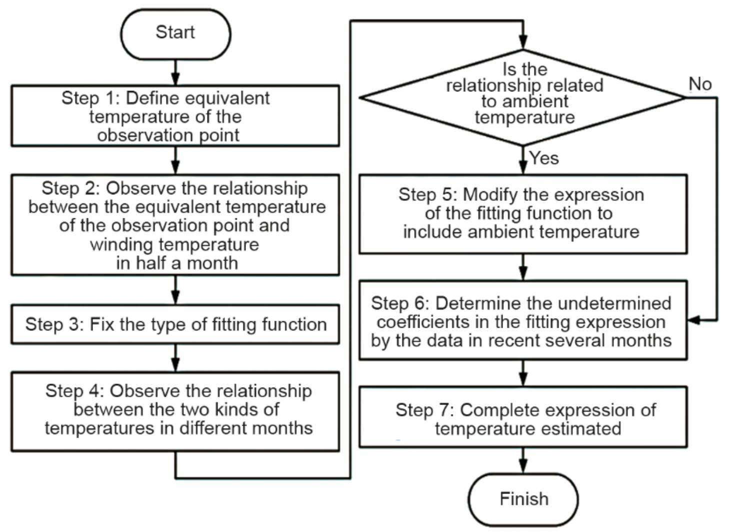

Figure 7. Flowchart of the proposed method

sensor that replaces the damaged one is installed at the end of the stator winding. Due to the symmetry of the stator structure of the hydrogenerator, the temperatures measured by the undamaged sensors should be approximately equal during normal operation of the hydrogenerator. Therefore, the mean value of these temperatures is taken as the equivalent temperature at the observation point, that is at the point of the damaged sensor:

$$T_{\mathrm{m}} = T_{\mathrm{avgm}} = \frac{1}{n}\sum_{i=1}^{n} T_{\mathrm{um}i} \tag{1}$$

where $T_{\mathrm{um}i}$ are the temperatures measured by the undamaged temperature sensors in the middle of the stator windings and n – the number of undamaged sensors. Based on the data-driven method, the relationship between T_{m} and the temperature measured by the new sensor installed at the end of the stator winding T_{e} is to be found, which is given by:

$$T_{\mathrm{m}} = f(T_{\mathrm{e}}) \tag{2}$$

Temperatures T_{m} and T_{e} *vs.* time in a period of time are shown in fig. 8. Unlike the relationship between the power and the temperature of stator winding, as shown in fig. 5, T_{m} and T_{e} always change simultaneously, *i.e.*, the relationship between them is independent of time, and there is only the simple algebraic operation, which is helpful to the real-time and accurate estimation of the observation point temperature of the hydrogenerator. Furthermore, because of the cooling type and structure of the hydrogenerator, T_{e} is always no higher than T_{m}, and both of them are always no lower than the ambient temperature. The relationship can be expressed:

$$T_0 \le T_{\mathrm{e}} \le T_{\mathrm{m}} \tag{3}$$

where T_0 is the ambient temperature, and both of equalities hold if and only if the hydrogenerator is completely cooled.

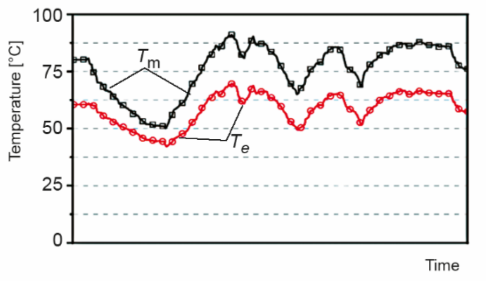

Figure 8. The T_m and T_e *vs.* time

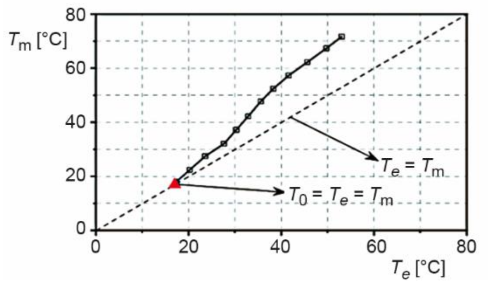

Figure 9. The T_m and T_e in the first half of January 2021

Periodically, all temperature sensors measure and record the current temperature simultaneously. The recorded data point (T_e, T_m) can be marked in the 2-D co-ordinates, fig. 9 gives the some measured data in the first half of Janunary 2021. It can be found that the curve $T_m = f(T_e)$ is always above the line $T_e = T_m$, which is in accordance with eq. (3). It also can be obtained from fig. 9 that the average ambient temperature in the first half of January 2021 is about 17 °C by eq. (3). According to the shape of the curve, the data of T_m and T_e can be fitted by using piecewise function, and each section is linear function, which helps to ensure the accuracy of the estimation and the simplicity of the algorithm. Thus, eq. (2) can be written:

$$T_m = \begin{cases} k_1 T_e + b_1 & T_e \in [T_0, T_0 + \Delta T_1) \\ k_2 T_e + b_2 & T_e \in [T_0 + \Delta T_1, T_0 + \Delta T_1 + \Delta T_2) \\ \vdots & \\ k_{n-1} T_e + b_{n-1} & T_e \in [T_0 + \sum_{i=1}^{n-2} \Delta T_i, T_0 + \sum_{i=1}^{n-1} \Delta T_i) \\ k_n T_e + b_n & T_e \in [T_0 + \sum_{i=1}^{n-1} \Delta T_i, +\infty) \end{cases} \tag{4}$$

where k_1, b_1, k_2, b_2, k_n, and b_n are coefficients of the fitting function and ΔT_i are the ranges of sections.

However, the ambient temperature T_0 can exert influence on the relationship between T_m and T_e. To illustrate this, fig. 10 shows T_m and T_e in the first half of January and August. In the northern hemisphere, generally, the ambient temperature in August is higher than that in January. Therefore, compared to the curve of January, the curve of August moved to the upper right. This means that different ambient temperatures need different coefficients of the fitting function eq. (4), which greatly increases the computational complexity and is difficult to implement. But it can be found that the curve shapes of these two months are very similar, *i.e.*, the two curves can be roughly overlapped by translation. Figure 11 shows the schematic diagram of translation, and the two curves coincide highly after translation. To better illustrate this, the temperature data for a year are analyzed. As the hydrogenerator is under maintenance in November, the temperature data for November cannot be provided. The temperature data for the first half of the recent 11 months are shown in fig. 12. Figure 12(a) shows the curves before translation while fig. 12(b) shows the curves after translation. The translation distance is determined by the ambient temperature of each month. As with the average ambient temperature of January, the average ambient temperatures of other 10 months can also be obtained through their respective curves. The average ambient temperatures in the first half of 11 months are given in tab. 2. The 11 curves of different months coincide well with each other after translation. Hence, after the introduction of ambient temperature T_0, coefficients of the fitting function do not need to change according to the change of T_0. Meanwhile, eq. (4) should be rewritten:

$$T_m = \begin{cases} k_1(T_e - T_0) + T_0 + b_1 & T_e \in [T_0, T_0 + \Delta T_1) \\ k_2(T_e - T_0) + T_0 + b_2 & T_e \in [T_0 + \Delta T_1, T_0 + \Delta T_1 + \Delta T_2) \\ \vdots \\ k_{n-1}(T_e - T_0) + T_0 + b_{n-1} & T_e \in [T_0 + \sum_{i=1}^{n-2} \Delta T_i, T_0 + \sum_{i=1}^{n-1} \Delta T_i) \\ k_n(T_e - T_0) + T_0 + b_n & T_e \in [T_0 + \sum_{i=1}^{n-1} \Delta T_i, +\infty) \end{cases} \tag{5}$$

In particular, $b_1 = 0$, which means $T_0 = T_e = T_m$ when the hydrogenerator is completely cooled.

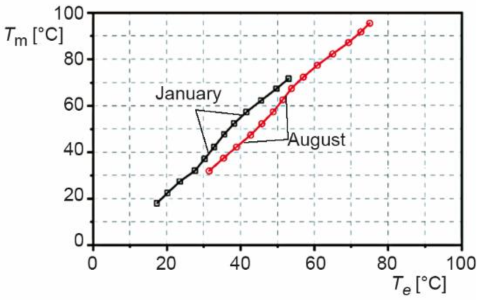

Figure 10. The T_m and T_e in the first half of January and August

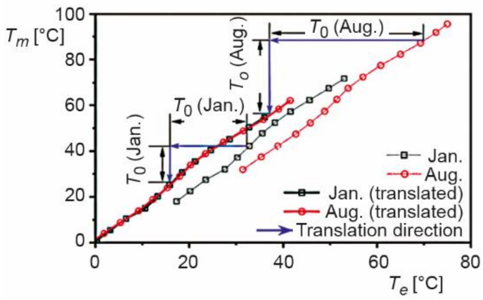

Figure 11. Translation of the two curves of January and August

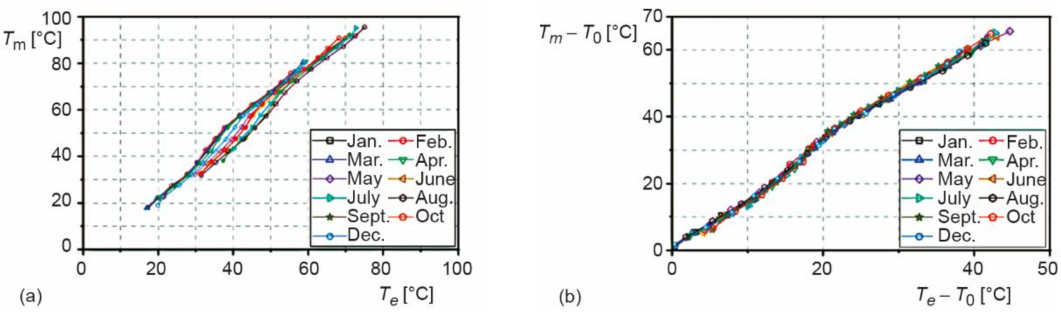

Figure 12. Temperature data for the first half of the recent 11 months; (a) before translation and (b) after translation

Table 2. Average ambient temperature in the first half of the recent 11 months

Month	T_0 [°C]	Month	T_0 [°C]
January	17	Feb.	17
March	17	Apr.	18
May	25	June	27
July	30	Aug.	33.5
September	32	Oct.	26
December	21	–	–

Table 3. Parameters of the fitting function

Parameters	Value	Parameters	Value	Parameters	Value
k_1	1.48	b_1	0	ΔT_1	9 °C
k_2	1.04	b_2	3.96	ΔT_2	2 °C
k_3	1.98	b_3	–6.37	ΔT_3	9 °C
k_4	2.17	b_4	–9.98	ΔT_4	2 °C
k_5	1.31	b_5	8.08	–	–

The shape of the 11 curves should be taken into consideration while choosing the number of sections of eq. (5) and the range of each section. If the number of sections is too small, the fitting function cannot accurately represent the original curves. On the contrary, too many sections will increase the complexity. Therefore, according to fig. 12, the number of sections is suitable for five, and the ranges of sections ΔT_i are given in tab. 3. The coefficients of the fitting function are obtained by linear fitting, as given in tab. 3.

The expression of estimated temperature in the middle of stator winding is:

$$T_{es} = \begin{cases} 1.48(T_e - T_0) + T_0 & T_e \in [T_0, T_0 + 9) \\ 1.04(T_e - T_0) + T_0 + 3.96 & T_e \in [T_0 + 9, T_0 + 11) \\ 1.98(T_e - T_0) + T_0 - 6.37 & T_e \in [T_0 + 11, T_0 + 19) \\ 2.17(T_e - T_0) + T_0 - 9.98 & T_e \in [T_0 + 19, T_0 + 21) \\ 1.31(T_e - T_0) + T_0 + 8.08 & T_e \in [T_0 + 21, +\infty) \end{cases} \tag{6}$$

where T_{es} is the estimated temperature in the middle of stator winding.

The image of the estimation function is shown in fig. 13. The expression of the estimation function varies with the different ambient temperatures, which is represented as translation on the curve, but the shape of the curve does not change. On the premise of knowing the ambient temperature and the end winding temperature, the observation point temperature can be estimated.

Ambient temperature

The ambient temperature, T_0, plays an indispensable part in the estimation. The ambient temperature can be obtained by adding a new temperature sensor, but this will increase the cost of the system and device. Therefore, a new way for obtaining T_0 without using the ambient temperature sensor is proposed. According to eq. (3), if the temperature of the end of the stator winding is very close to the temperature of the middle of the stator winding, the temperature of the end of the stator winding should be also close to the ambient temperature. The expression can be given by:

$$\left| T_\mathrm{e} - \frac{1}{n}\sum_{i=1}^{n} T_{\mathrm{um}i} \right| < \delta T \tag{7}$$

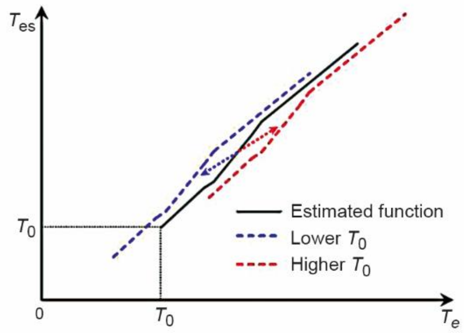

Figure 13. Estimation function

where δT denotes the maximum permissible temperature difference. The value of δT can be set to 0.5 °C or a less value. The two ways of obtaining ambient temperature are shown in fig. 14. Though the later way cost less than the former way, the accuracy and timeliness of the later way is not as good as the former way. Hence, to ensure the accuracy of the estimation, the way by using the ambient temperature sensor is preferred.

Figure 14. Two ways of obtaining ambient temperature

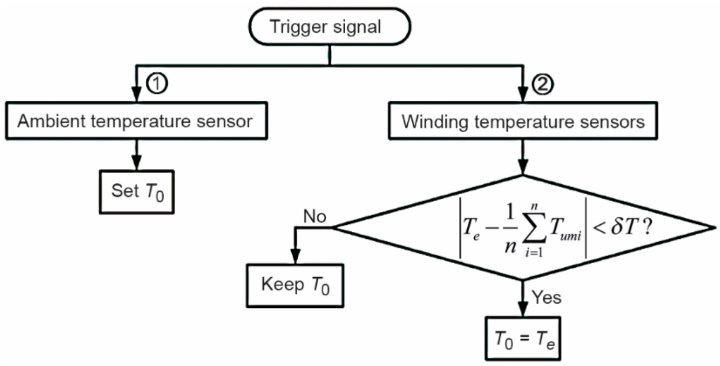

Real-time temperature

The temperature measurement system of the hydrogenerator is shown in fig. 15. This system includes a hydrogenerator, an optical fibre temperature measuring, a temperature measuring brake screen, an upper-computer, and a display screen. The working principle of this system is illustrated. The temperature of the stator winding is measured by the temperature sensor. Then, the temperature is transmitted to the demodulator via optical fiber and the digital quantity of temperature is got. Finally, the digital quantity is passed to the host through RS485 communication and shown in the display screen. When the temperature of stator winding is greater than the set value, the hydrogenerator

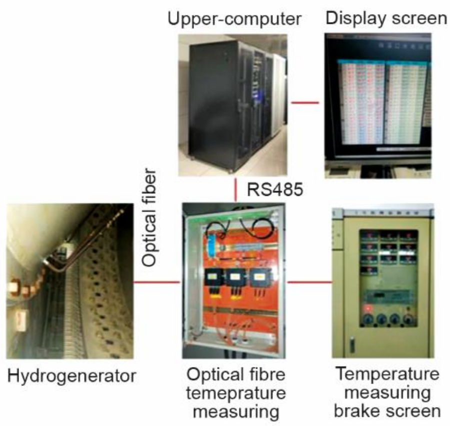

Figure 15. Overall structure of temperature measurement system

would be braked and the information would be displayed on the temperature measuring brake screen.

In order to clearly observe the installation position of the temperature sensor, the partial drawing of stator winding end is given in fig. 16. Figure 16(a) gives the end of stator winding. Figure 16(b) shows that a temperature sensor is installed on the surface of the stator winding end, which is wrapped by glass ribbon.

Figure 17 gives the output power and temperature curves shown on the displayer. It can be found that the temperature of the stator winding changed with the output power, but their changes were not simultaneous due to the temperature inertia.

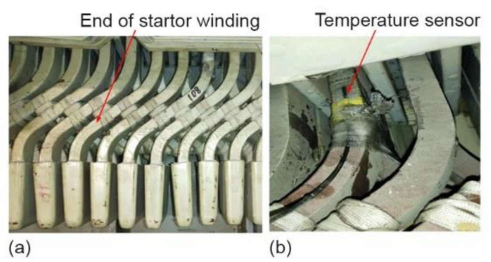

Figure 16. Temperature measurement; (a) stator winding end and (b) installation of temperature sensor

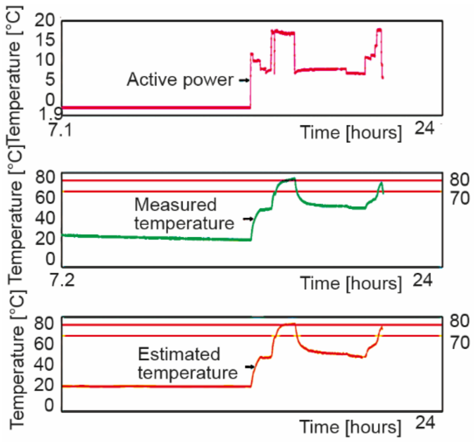

Figure 17. Output power and temperature on the display screen; (a) active power, (b) measured temperature, and (c) estimated temperature

Figure 18 gives the estimated and measured temperatures under different four days. It can be found that the temperature of the stator winding was always fluctuating throughout the day. Meanwhile, the proposed method can estimate the temperature in the middle of stator winding of the hydrogenerator well regardless of whether it was high or low.

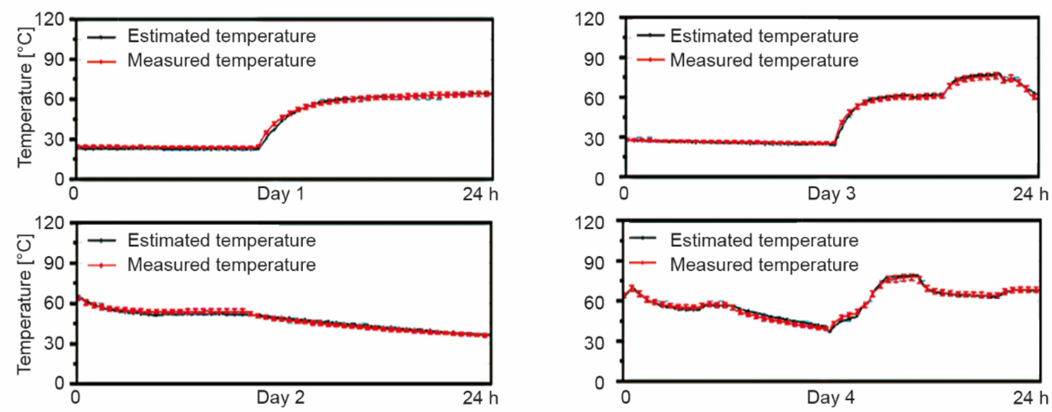

Figure 18. Estimated and measured temperatures under different four days

Conclusion

A novel and simple method is proposed and validated for estimating the real-time temperature of stator winding of the air-cooled hydrogenerator. The relationship between the output power and real-time temperature is analyzed. It can be found that the real-time temperature cannot be directly obtained through the output power due to the inertia of temperature. To estimate the real-time temperature, a data-driven method for estimating the stator winding temperature is proposed and implemented. The method is tested on an 18.5 MW air-cooled hydrogenerator, and the experimental data proves the effective of the proposed method. This method is simple and reliable, and provides a new idea for the temperature monitoring of large hydrogenerators.

References

[1] Wang, P., *et al.*, Robustness Improvement on PMU Based Dynamic Equivalent Modeling of Distributed Small Hydropower Generator Stacks, *IEEE Transactions on Power Systems*, *35* (2020), 5, pp. 3388-3399
[2] Han, J., *et al.*, Thermal Modeling and Experimental Validation in the Rotor Region of Hydrogenerator With Different Rotor Structures, *IEEE Access*, *9* (2021), July, pp. 120001-120009
[3] Sumereder, C., Statistical Lifetime of Hydro Generators and Failure Analysis, *IEEE Transactions on Dielectrics and Electrical Insulation*, *15* (2008), 3, pp. 678-685
[4] Hwang, S.-W., *et al*, Design Process and Verification of SPMSM for a Wearable Robot Considering Thermal Characteristics Through LPTN, *IEEE/ASME Transactions on Mechatronics*, *26* (2021), 2, pp. 1033-1042
[5] Tong, W., *et al.*, Loss and Thermal Analysis for High-Speed Amorphous Metal PMSMs Using 3D Electromagnetic-Thermal Bi-Directional Coupling, *IEEE Transactions on Energy Conversion*, *36* (2021), 4, pp. 2839-2849
[6] Tosetti, M., *et al.*, Conjugate Heat Transfer Analysis of Integrated Brushless Generators for More Electric Engines, *IEEE Transactions on Industry Applications*, *50* (2014), 4, pp. 2467-2475
[7] Tovar-Barranco, A., *et al.*, Modeling of End-Space Convection Heat-Transfer for Internal and External Rotor PMSMs With Fractional-Slot Concentrated Windings, *IEEE Transactions on Industrial Electronics*, *68* (2021), 3, pp. 1928-1937
[8] Boglietti, A., *et al.*, Evolution and Modern Approaches for Thermal Analysis of Electrical Machines, *IEEE Transactions on Industrial Electronics*, *56* (2009), 3, pp. 871-882
[9] Dong, B., *et al.*, Thermal Analysis and Experimental Validation of a 30 kW 60000 r/min High-Speed Permanent Magnet Motor With Magnetic Bearings, *IEEE Access*, *7* (2019), July, pp. 92184-92192
[10] Bäuml, T., *et al.*, An Innovative Parametrization Method for a Thermal Equivalent Circuit Model of an Interior Permanent Magnet Synchronous Machine, *Proceedings*, IECON 2011 – 37th Annual Conference of the IEEE Industrial Electronics Society, Melbourne, Australia, 2011, pp. 1746-1751
[11] Weili, L., *et al.*, Influence of Rotation on Rotor Fluid and Temperature Distribution in a Large Air-Cooled Hydrogenerator, *IEEE Transactions on Energy Conversion*, *28* (2013), 1, pp. 117-124
[12] ***, http://www.sgzhongli.com/html/product1.html
[13] Phuc, P. N., *et al*, Rotor Temperature Virtual Sensing for Induction Machines Using a Lumped-Parameter Thermal Network and Dual Kalman Filtering, *IEEE Transactions on Energy Conversion*, *36* (2021), 3, pp. 1688-1699

Paper submitted: February 24, 2022
Paper revised: May 23, 2022
Paper accepted: June 22, 2022